High-Fat Diet–Induced Obesity Promotes Expansion of Bone Marrow Adipose Tissue and Impairs Skeletal Stem Cell Functions in Mice

Tencerova, Michaela; Figeac, Florence; Ditzel, Nicholas; Taipaleenmäki, Hanna; Nielsen, Tina Kamilla; Kassem, Moustapha

Published in:
Journal of Bone and Mineral Research

DOI:
10.1002/jbmr.3408

Publication date:
2018

Document version
Publisher's PDF, also known as Version of record

THE MORE YOU IMAGE THE MORE YOU UNDERSTAND

Quantum GX2 microCT

Automate bone mineral density calculations.

Without question, microCT is the go-to modality for bone imaging, and bone-research applications such as osteoarthritis and osteoporosis use bone mineral density (BMD) as a readout for the disease state. Discover how the Quantum GX2 microCT imaging system and AccuCT™ advanced bone-analysis software can be used to automatically calibrate BMD scans, saving you time, while improving consistency across analyses.

Download Technical Note

PerkinElmer®
For the Better

ORIGINAL ARTICLE

JBMR®

High-Fat Diet–Induced Obesity Promotes Expansion of Bone Marrow Adipose Tissue and Impairs Skeletal Stem Cell Functions in Mice

Michaela Tencerova,[1,2*] Florence Figeac,[1*] Nicholas Ditzel,[1] Hanna Taipaleenmäki,[3] Tina Kamilla Nielsen,[1] and Moustapha Kassem[1,4,5]

[1]Department of Molecular Endocrinology, KMEB, University of Southern Denmark and Odense University Hospital, Odense C, Denmark
[2]Danish Diabetes Academy, Odense C, Denmark
[3]Molecular Skeletal Biology Laboratory, Department of Trauma, Hand, and Reconstructive Surgery, University Medical Center Hamburg-Eppendorf, Hamburg, Germany
[4]Department of Cellular and Molecular Medicine, Danish Stem Cell Center (DanStem), University of Copenhagen, Copenhagen, Denmark
[5]Stem Cell Unit, Department of Anatomy, Faculty of Medicine, King Saud University, Kingdom of Saudi Arabia

ABSTRACT

Obesity represents a risk factor for development of insulin resistance and type 2 diabetes. In addition, it has been associated with increased adipocyte formation in the bone marrow (BM) along with increased risk for bone fragility fractures. However, little is known on the cellular mechanisms that link obesity, BM adiposity, and bone fragility. Thus, in an obesity intervention study in C57BL/6J mice fed with a high-fat diet (HFD) for 12 weeks, we investigated the molecular and cellular phenotype of bone marrow adipose tissue (BMAT), BM progenitor cells, and BM microenvironment in comparison to peripheral adipose tissue (AT). HFD decreased trabecular bone mass by 29%, cortical thickness by 5%, and increased BM adiposity by 184%. In contrast to peripheral AT, BMAT did not exhibit pro-inflammatory phenotype. BM progenitor cells isolated from HFD mice exhibited decreased mRNA levels of inflammatory genes (*Tnfα*, *IL1β*, *Lcn2*) and did not manifest an insulin resistant phenotype evidenced by normal levels of pAKT after insulin stimulation as well as normal levels of insulin signaling genes. In addition, BM progenitor cells manifested enhanced adipocyte differentiation in HFD condition. Thus, our data demonstrate that BMAT expansion in response to HFD exerts a deleterious effect on the skeleton. Continuous recruitment of progenitor cells to adipogenesis leads to progenitor cell exhaustion, decreased recruitment to osteoblastic cells, and decreased bone formation. In addition, the absence of insulin resistance and inflammation in the BM suggest that BMAT buffers extra energy in the form of triglycerides and thus plays a role in whole-body energy homeostasis. © 2018 The Authors. *Journal of Bone and Mineral Research* Published by Wiley Periodicals, Inc.

KEY WORDS: HIGH-FAT DIET–INDUCED BONE LOSS; BONE MARROW ADIPOSE TISSUE; BONE MARROW SKELETAL STEM CELLS; INSULIN SENSITIVITY; INFLAMMATION

Introduction

Obesity is a major health problem worldwide and represents a significant risk factor for insulin resistance, type 2 diabetes (T2D), and cardiovascular diseases.[1] Recent epidemiological studies have reported an association between obesity and increased risk of fragility fractures.[2] However, the biological mechanisms underlying this phenomenon are not known.

In addition to the expansion of peripheral adipose tissue (AT) in obesity, a similar expansion in bone marrow adipose tissue (BMAT) takes place.[3,4] BMAT is a newly recognized endocrine-active fat depot that is present in the non-hematopoietic marrow and in close contact with hematopoietic and bone tissues.[5,6] BMAT responds to metabolic needs of the organism as evidenced by significant expansion in a number of pathophysiological conditions, e.g., aging, diabetes, obesity, and anorexia nervosa or during pharmacological treatment with thiazolidinediones, glucocorticoids, or chemotherapy.[3,4,7–9] BMAT originates from the bone marrow skeletal (also known as stromal or mesenchymal) stem cells (BM-MSC) present in the bone marrow (BM) stroma. BM-MSC give rise, in addition to adipocytes, to osteoblasts and hematopoietic-supporting stroma.[9] The differentiation capacity of BM-MSC is regulated via several secreted factors (e.g., sFRP-1, Dlk1/Pref-1), immune molecules (e.g.,

Received in original form November 7, 2017; revised form February 8, 2018; accepted February 9, 2018. Accepted manuscript online February 14, 2018.
Address correspondence to: Michaela Tencerova, PhD, Department of Molecular Endocrinology, KMEB, University of Southern Denmark and Odense University Hospital, DK-5000 Odense C, Denmark. E-mail: mtencerova@health.sdu.dk
*MT and FF contributed equally to this work.
Additional Supporting Information may be found in the online version of this article.
Journal of Bone and Mineral Research, Vol. 33, No. 6, June 2018, pp 1154–1165
DOI: 10.1002/jbmr.3408

interleukins, TNFα,[10] microRNAs[11]), and systemic hormones (e.g., parathyroid hormone[12] and insulin-like growth factors[13]) present within the BM-MSC niche, which dictate lineage fate.[5,14,15] Moreover, BM-MSC lie in the vicinity of hematopoietic stem cells (HSC), whose microenvironment is affected in obesity and thus may participate in the regulation of BM-MSC differentiation and bone homeostasis.[16–19] However, the possible relationship between increased BM adiposity, bone mass, and bone fragility are not completely determined.

Despite increased attention on the regulation of bone versus fat formation in the BM as a regulatory factor for bone formation, little is known regarding the metabolic function of BMAT and its contribution to whole-body energy metabolism. Although there is extensive literature on the role of visceral, subcutaneous, and brown adipose depots (VAT, SAT, BAT, respectively) in the development of insulin resistance and T2D, few studies have investigated the function of BMAT as an adipose storage organ.[6,8,20,21] In obesity and T2D, peripheral AT develops insulin resistance and exhibits impaired insulin signaling.[22] However, there is no clear information about insulin sensitivity in BMAT.[23,24]

In the current study, we hypothesized that obesity leads to metabolic changes in the BM microenvironment affecting BM-MSC biology, BMAT phenotype, and skeletal homeostasis. Using a mouse model of high-fat diet (HFD)–induced obesity, we investigated changes in bone mass, bone marrow fat mass, as well as the molecular phenotype and insulin sensitivity of BMAT and BM-MSC as compared with peripheral AT. We demonstrated that in response to HFD, there is an expansion in BMAT volume that is associated with decreased bone mass and impaired differentiation of BM-MSC.

Materials and Methods

Additional procedures are described in the Supplemental Data.

Animals

Male C57BL/6J mice (Taconic, Rensselaer, NY, USA) were given ad libitum normal chow diet (Altromin [Lage, Germany] 132003, containing 6% fat, 30% protein, 63% carbohydrate, 7.7% sucrose) or 60 kcal% high-fat diet (Research Diet [New Brunswick, NJ, USA] D12492, containing 35% fat, 26% protein, 26% carbohydrate, 8.8% sucrose) at 8 weeks of age for a period of 12 or 20 weeks. Animals were bred and housed under standard conditions (21°C, 55% relative humidity) on a 12-hour light/dark cycle. All experimental procedures were approved by the Danish Animal Ethical committee (2017-15-0201-01210).

Micro-computed tomography scanning (μCT)

Proximal tibias of mice fed for 12 weeks with HFD or with normal diet (ND) as control were scanned with a high-resolution μCT system (vivaCT40; Scanco Medical, Bassersdorf, Switzerland), resulting in three-dimensional (3D) reconstruction of cubic voxel sizes $10.5 \times 10.5 \times 10.5\ \mu m^3$. A detailed description for the quantification of 3D microarchitecture of trabecular and cortical bone has been presented previously.[25]

Isolation of bone marrow skeletal stem cells (BM-MSC) and hematopoietic stem cells (HSC)

BM-MSC were isolated from the bones of front and hind limbs of C57BL/6J male mice (after 12 weeks of HFD) following the protocol of Zhu and colleagues and Houlihan and colleagues[26,27] with a slight modification. After bone crushing, a collagenase digestion (StemCell, Vancouver, Canada; 5% collagenase) and negative selection of CD45, CD31, and Ter119 cells was done to obtain BM-MSC. The positive fraction with hematopoietic stem cells (HSC) was also kept for further analysis. Cells were cultivated and expanded *in vitro* up to passage 3. The BM-MSC were pooled from 2 mice in each group and used for subsequent analyses.

Isolation of bone marrow adipose tissue (BMAT)

BMAT were isolated from long bones based on the protocol of Liu and colleagues and Lanske and colleagues by flushing the BM, quick high-speed spinning, and removing HSC.[28,29] Then the pellets containing the BMAT and HSC were resuspended in phosphate buffered saline (PBS) to let BMAT float on the top of the liquid suspension. HSC pellet was lysed with erythrocyte lysis buffer to remove red blood cells.

Isolation of adipose-derived stromal (mesenchymal) stem cells (AT-MSC)

Epididymal fat pads were mechanically dissociated using the gentleMACS Dissociator (Miltenyi Biotec, Bergisch Gladbach, Germany) and collagenase digested at 37°C for 45 minutes in HBSS (Gibco, Life Technologies, Carlsbad, CA, USA) containing 2% BSA (American Bioanalytical, Natick, MA, USA) and 1% collagenase (Sigma-Aldrich, St. Louis, MO, USA). Samples were filtered through 300-μm-diameter pore nylon mesh and centrifuged. The adipocyte layer and the supernatant were aspirated and the pelleted cells were collected as the stromal-vascular fraction (SVF) containing AT-MSC. The cells were then treated with red blood cell lysis buffer and washed with PBS and plated or directly harvested for further analysis. The cells were then plated at a density of 200,000 cells/well in 6-well plates.

Dynamic bone histomorphometry

Mice were injected with calcein 30 mg/kg (Fluka Chemie, Buchs, Switzerland) at 9 and 2 days, respectively, before euthanasia. OsteoMeasure analysis software (OsteoMetrics, Decatur, GA, USA) was used to evaluate mineral apposition rate (MAR) (in mm/d) in the frozen sections of tibia and vertebrae according to standard protocols.[30,31]

Results

HFD-induced obesity decreased trabecular and cortical bone mass

To determine the effect of obesity on BMAT and bone metabolism, C57BL/6J male mice were fed with a high-fat diet (HFD) (60% kcal of fat) for 12 weeks. After 12 weeks, HFD mice exhibited increased body weight (29%), body fat mass (212%), and impaired glucose tolerance compared with normal chow diet mice (ND) (Supplemental Fig. S1*A–D*).

μCT of proximal tibia showed decreased trabecular bone volume per total volume (BV/TV) and trabecular number (Tb.N), and increased trabecular separation (Tb.Sep), whereas trabecular thickness (Tb.Th) was unchanged in HFD mice compared with ND mice (Fig. 1*A*). Similarly, cortical bone parameters BV/TV and thickness were reduced in HFD mice at diaphysis (Fig. 1*B*) but unchanged at metaphysis. No change in periosteal circumference was detectable (Supplemental Fig. S2*A–D*). These changes are demonstrated in representative 3D reconstruction images of trabecular and cortical bone in ND and HFD mice (Fig. 1*C*).

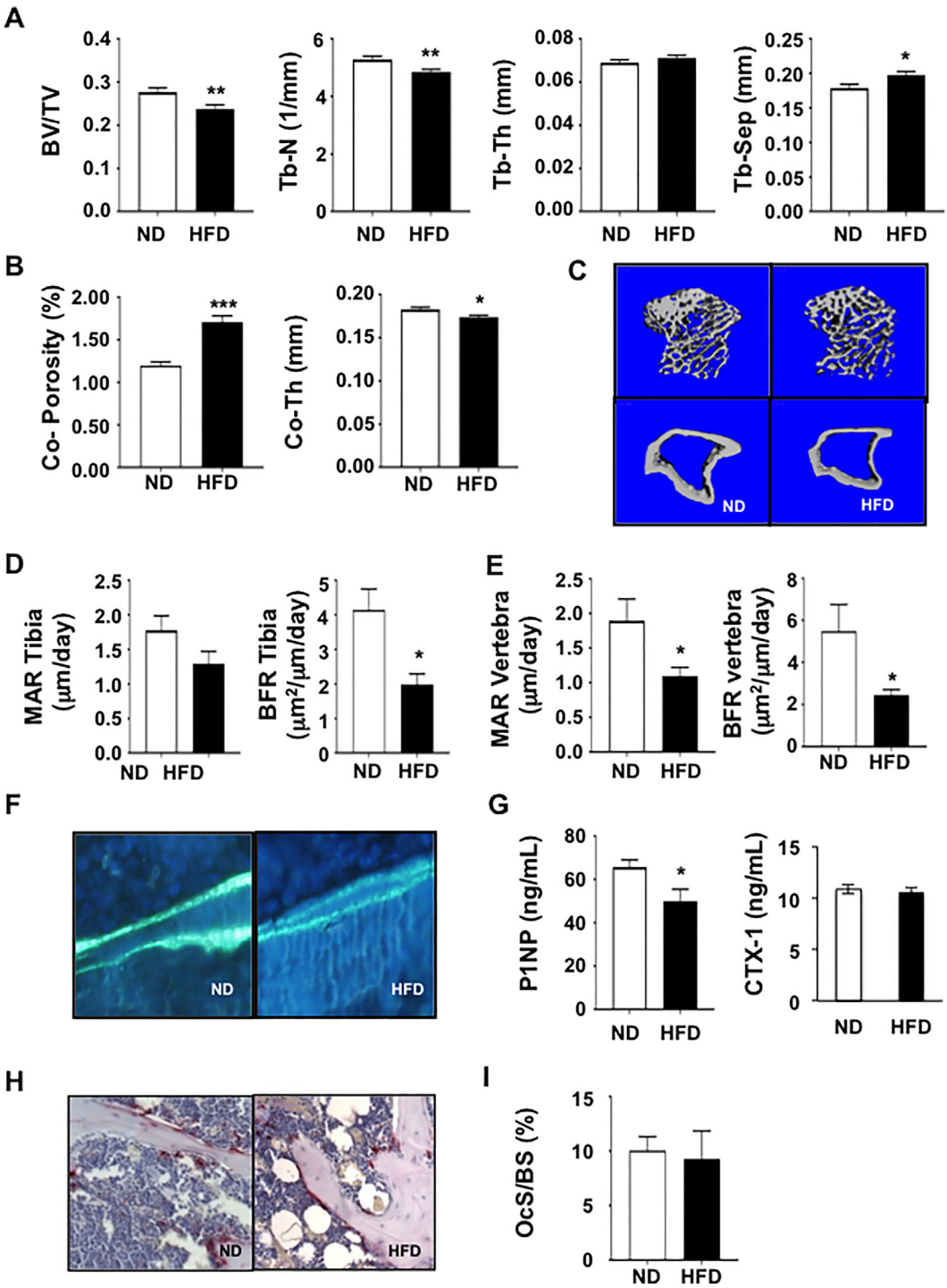

Fig. 1. Bone phenotype of HFD mice. (*A–C*) µCT analysis of proximal tibia after 12 weeks of HFD and ND as a control. (*A*) At metaphysis, trabecular bone parameters were evaluated as bone volume per total volume (BV/TV), trabecular number (Tb.N), trabecular thickness (Tb.Th), and trabecular separation (Tb.Sep). (*B*) µCT analysis of cortical diaphysis bone measurements was evaluated as cortical BV/TV (Co.BV/TV) and cortical thickness (Co.Th). (*C*) Representative images for µCT 3D reconstruction of trabecular (upper panel) and cortical (lower panel) compartments. Data are presented as mean ± SEM ($n = 32$), $^{*}p < 0.05$, $^{**}p < 0.01$; $^{***}p < 0.001$: ND versus HFD. (*D*) Quantification of double calcein labeling of trabecular bone in tibia: mineral apposition rate (MAR) (left panel) calculated from the distance between the two labeled layers and bone formation rate (BFR) (right panel) calculated as a function of daily MAR and (*E*) in vertebrae, respectively, left and right panel from ND and HFD groups ($n = 6$ per group). (*F*) Representative pictures of double calcein labeling of vertebrae from animals fed with ND and HFD for 12 weeks. (*G*) Markers for bone turnover, P1NP ($n = 15$ per group) for bone formation (left panel) and CTX-1 ($n = 9$ per group) for bone resorption (right panel) were measured in serum. (*H*) Histomorphometric analysis on bone sections from ND and HFD tibia (representative sections) after 12 weeks of diet stained with tartrate-resistant acid phosphatase (TRAP) ($n = 6$). (*I*) Osteoclast surface per bone surface (OcS/BS%) was evaluated in tibia. Data are presented as mean ± SEM; $^{*}p < 0.05$: ND versus HFD; two-tailed unpaired Student's *t* test.

Dynamic bone histomorphometry performed on tibia and vertebrae showed a trend toward decreased mineral apposition rate (MAR) and a significant decrease in bone formation rate (BFR) in tibia, whereas both parameters were significantly reduced in the vertebrae of HFD mice (Fig. 1*D–F*). Moreover, serum levels of bone formation marker procollagen type 1 N-terminal propeptide (P1NP) decreased, but bone resorption marker C-telopeptide of type I collagen (CTX-1) did not change in HFD mice (Fig. 1*G*). Similarly, histological analyses of proximal tibia sections using tartrate-resistant acid phosphatase (TRAP) staining (Fig. 1*H*) showed no changes in osteoclasts surface per total bone surface (Fig. 1*I*) or number of osteoclasts per total bone surface (data not shown), suggesting that the osteoclast activity did not change with HFD.

Bone marrow adipose tissue (BMAT) volume increased in HFD-induced obesity

To evaluate BMAT volume, BMAT was visualized by osmium-tetraoxide staining in long bones (tibias) ex vivo after 12 weeks of HFD. Histological sections of osmium-stained bones demonstrated the strong affinity of the osmium for BMAT (Fig. 2*A*). μCT imaging of osmium tetroxide-stained BMAT revealed increased BMAT volume in tibia, especially in the proximal metaphysis and in the distal diaphysis (Fig. 2*B–D*). In ND mice, most of the BMAT was present in distal tibia (Fig. 2*D*). Further, histomorphometric analysis of hematoxylin-eosin-stained sections of the bones confirmed a significant increase of BM adiposity in proximal tibia in HFD mice (Fig. 2*E*, *F*). These changes in the BM were accompanied by increased BM adipocyte number and size (adipocyte area) (Fig. 2*G*, *H*). Perilipin staining, a specific marker of adipocytes, localized the area of adipocytes (Fig. 2*I*). In addition, in the whole group of mice, tibia BMAT volume was negatively correlated with BV/TV and Tb.N and positively correlated with Tb.Sep (Supplemental Fig. S3*A–C*).

HFD-induced obesity altered BM-MSC stemness and differentiation

To determine the cellular mechanisms of enhanced adipogenesis and decreased bone mass in obese mice, we first examined the cellular and molecular phenotype of BM-MSC. HFD reduced the percentage of CD73+ and Sca1/CD140a+ cells in BM-MSC (Fig. 3*A*) assuming that the proportion of progenitor populations changed. The short-term proliferation rate and colony-forming units-fibroblast (CFU-f) of primary cultures were decreased in HFD mice (Fig. 3*B*, *C*). We did not find evidence for increased number of senescent cells stained positive for senescence-associated β-galactosidase, nor for increased levels of senescent gene markers (*p16*, *p21*) in BM-MSC cultures of HFD mice (Fig. 3*D*, *E*). Further, BM-MSC obtained from HFD mice exhibited increased adipocytic (AD) differentiation capacity compared with ND mice measured by mRNA gene expression of adipogenic genes, ie, *Pparγ2, Lep, Adipoq, Fsp27* (Fig. 3*F*). Osteoblast (OB) differentiation of BM-MSC obtained from HFD mice revealed increased alkaline phosphatase (ALP) activity (Fig. 3*G*). mRNA levels of specific osteoblastic genes (ie, *Alp, Runx2, Ocn*) did not show differences of BM-MSC in HFD mice compared with ND (Fig. 3*H*).

HFD-induced obesity did not lead to a pro-inflammatory BM microenvironment

To investigate the mechanism underlying the BM-MSC changes in lineage commitment, we examined changes in BM microenvironment. Because obesity is associated with increased inflammation in peripheral AT, we examined whether obesogenic condition in mice has a similar effect on BM microenvironment. Immunophenotyping showed an altered composition of immune cells in BM with decreased number of CD19+ B cells and increased number of CD4+ T lymphocytes as well as CD45+ hematopoietic cells in HFD mice (Fig. 4*A*). However, mRNA levels of inflammatory gene markers in HSC revealed decreased inflammatory signature in BM under HFD condition evidenced by decreased mRNA expression of *Il1β,* which was more manifested after 20 weeks of HFD by decreased mRNA levels of *Il6* and Lipocalin 2 (*Lcn2*) in addition to *Il1β* (Supplemental Fig. S4*A*, *B*). To confirm the low pro-inflammatory phenotype, isolated CD45+ hematopoietic cells exposed to lipopolysaccharide (LPS) exhibited decreased inflammatory response measured by mRNA levels of *Il1β* and *Mcp1* in HFD mice compared with ND mice (Fig. 4*C*). In addition, the response to LPS stimulation was similar in HFD compared with ND mice with a respect to activation of NF-κB pathway, one of the key inflammatory pathways, as measured by phospho IκBα and p65 activity (Fig. 4*D*).

HFD-induced obesity did not exhibit a pro-inflammatory phenotype of BMAT compared with peripheral adipose tissue (AT)

Changes in BM microenvironment in response to HFD can be mediated by the accumulated BMAT. Thus, we characterized the molecular phenotype of BMAT isolated from long bones in response to HFD-induced obesity and compared to visceral adipose tissue (VAT) with known pro-inflammatory phenotype as well as brown adipose tissue (BAT). Under basal conditions of ND, the gene expression profile of BMAT showed higher mRNA levels of pro-inflammatory genes (*Tnfα*, *Il1β*, and *Lcn2*) compared with peripheral adipose depot: VAT and BAT (Fig. 5*A*). In contrast, genes related to insulin signaling (*Insr, Irs1, Igf1*) and adipogenesis (*Pparγ2, Ap2, Adipoq, Lep*) were highly expressed in VAT and BAT compared with BMAT (Fig. 5*B*, *C*). Molecular signature of BMAT was different from BAT except for *Dio2*, which showed similar mRNA levels in BMAT and BAT (Fig. 5*D*).

In HFD, BMAT manifested increased gene expression of insulin signaling genes (*Insr*), adipogenic genes (*Adipoq, Lep, Fsp27, C/ebpα*), and decreased pro-inflammatory genes (*Lcn2*) (Supplemental Fig. S4*B*), which was opposite to the phenotype observed in VAT with decreased mRNA levels of insulin signaling genes (*Irs1, Irs2, Insr*), adipogenic genes (*Adipoq, Fsp27, Cidea, C/ebpα, Pparγ2*), and increased mRNA levels of pro-inflammatory genes (*Tnfα, Il1β, and Lcn2*) (Supplemental Fig. S4*C*). Similar results with a more pronounced phenotype in BMAT and VAT were observed after 20 weeks of HFD (Fig. 5*E*, *F*).

HFD-induced obesity did not impair insulin sensitivity in BM-MSC compared with AT-MSC

Insulin resistance accompanies HFD-induced obesity and may play a role in mediating changes in BM-MSC niche. To test this hypothesis, we examined insulin signaling and responsiveness in BM-MSC obtained from HFD mice and compared with AT-MSC derived from VAT previously shown to exhibit insulin resistance and inflammation in HFD-induced obesity.[32] In HFD mice, VAT AT-MSC exhibited impaired adipocytic (AD) differentiation (Supplemental Fig. S5*A*, *B*) and under basal conditions decreased gene expression of *Pparγ2* and increased mRNA levels of *Tnfα,* a marker of inflammatory status in AT. On

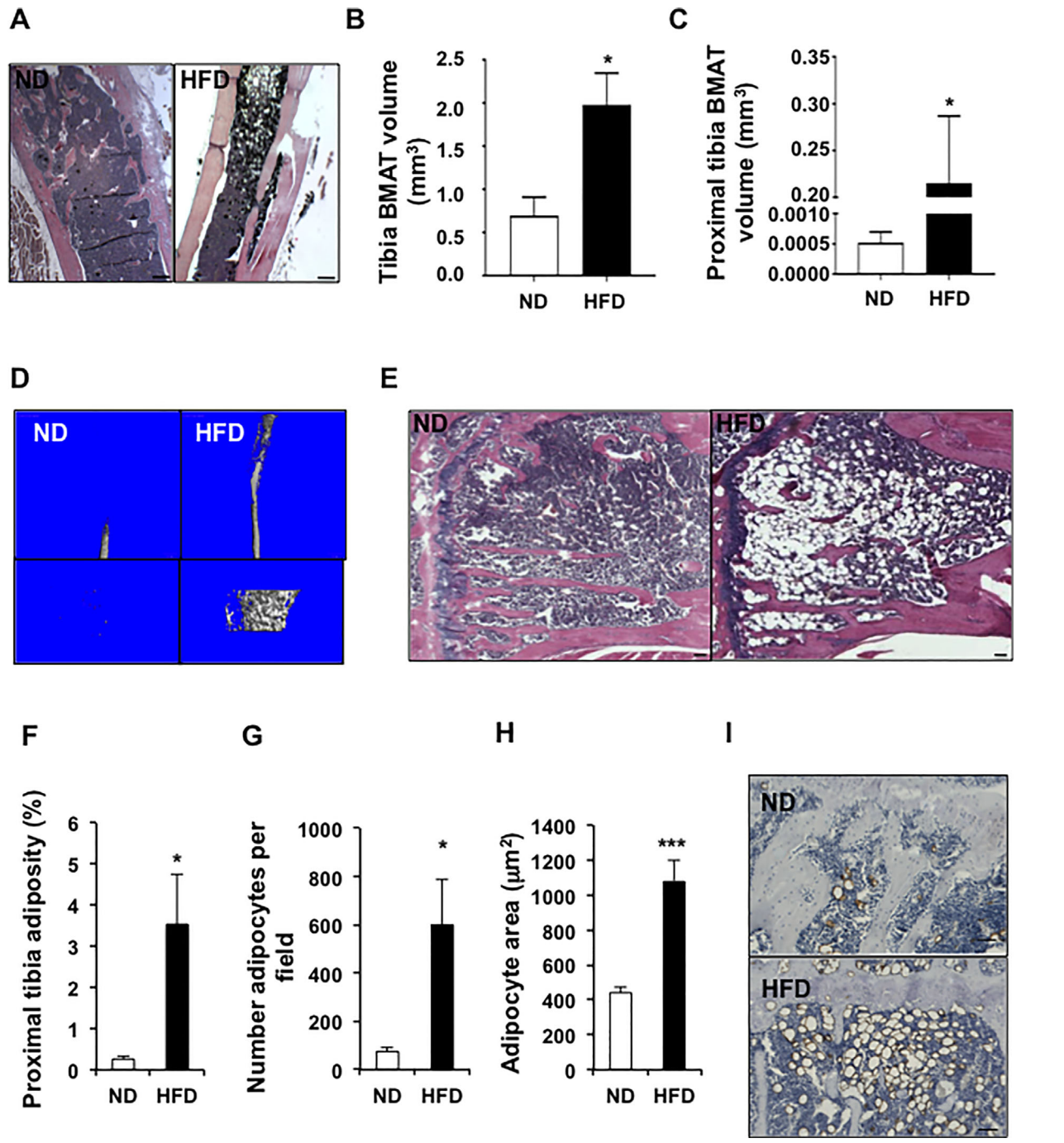

Fig. 2. BMAT evaluation in HFD mice. (*A*) Histological sections of tibia after osmium staining and stained with H&E. Black = adipocytes stained by osmium; scale bar = 100 μm. (*B–D*) Quantification of the bone marrow adipose tissue (BMAT) volume in (*B*) full-length tibia (all marrow cavity) and (*C*) proximal tibia area (previously evaluated for trabecular parameters) evaluated by μCT from osmium-stained bones. (*D*) Representative images of μCT 3D reconstruction of BMAT from full-length tibia (upper panel) and proximal tibia area (lower panel) of mice fed for 12 weeks with ND or HFD. (*E*) H&E staining of histological sections of tibia from mice fed for 12 weeks with ND or HFD; scale bar = 100 μm. (*F–H*) Histomorphometric evaluation of the BMAT expressed as (*F*) adiposity (adipocytes surface per field), (*G*) adipocytes number per field, and (*H*) adipocyte area on H&E sections. (*I*) Perilipin staining of histological tibia sections from mice fed for 12 weeks with ND or HFD. Scale bars = 100 μm. Data are presented as mean ± SEM ($n = 6$ per group); $^{*}p < 0.05$, $^{**}p < 0.01$: ND versus HFD, two-tailed unpaired Student's *t* test.

the other hand, BM-MSC exhibited increased gene expression of *Pparγ2* and decreased gene expression of *Tnfα* (Fig. 6*A*, *B*), suggesting the opposite metabolic phenotype. In addition, under HFD insulin-stimulated activation of pAKT(S473)/totalAKT was decreased in undifferentiated and AD differentiated progeny in VAT AT-MSC, whereas BM-MSC maintained insulin responsiveness under basal and following AD differentiation (Fig. 6*C–F*).

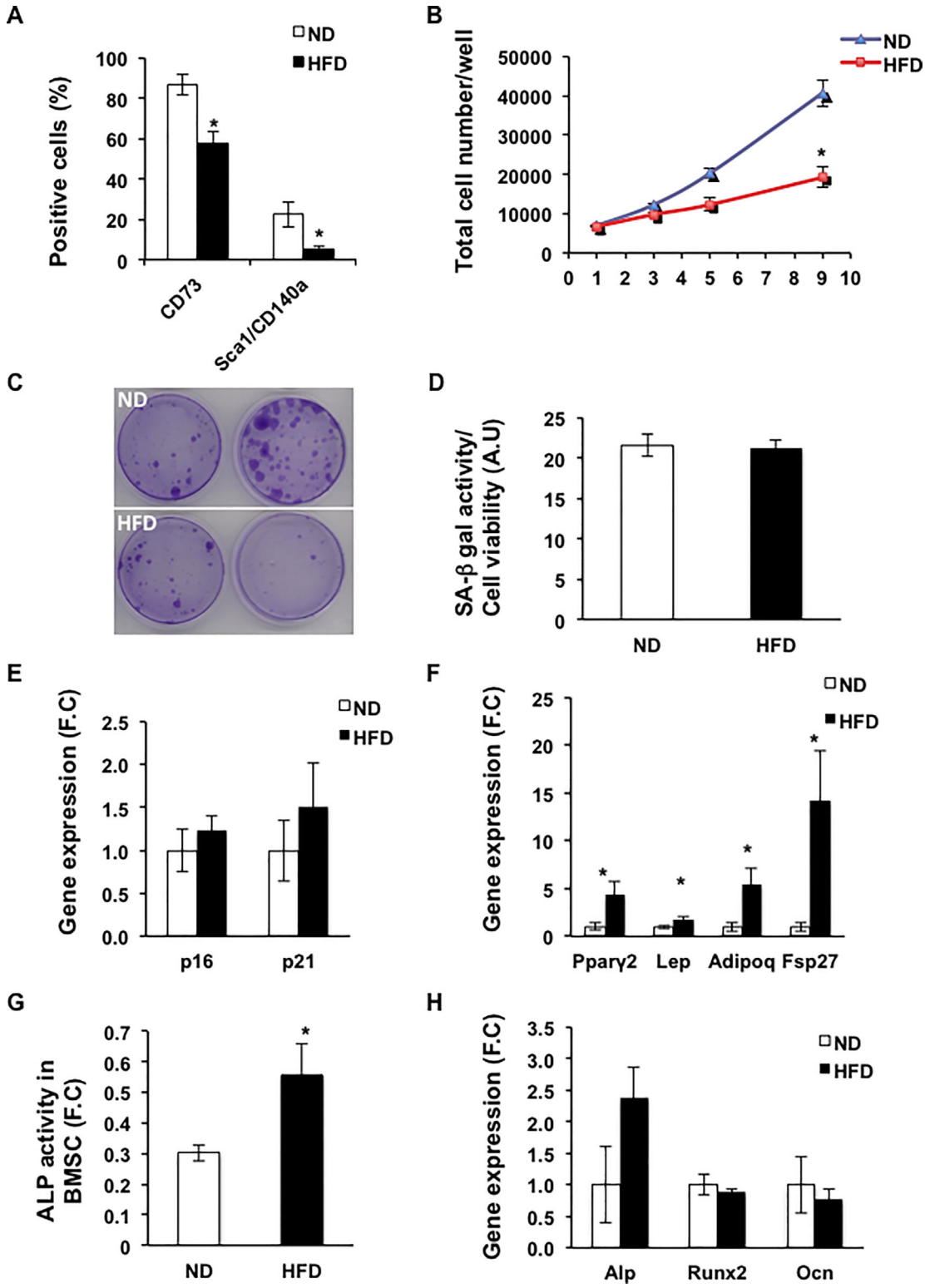

Fig. 3. Molecular and cellular characteristics of BM-MSC in HFD mice. Primary bone marrow skeletal stem cells (BM-MSC) isolated from mice fed for 12 weeks with ND or HFD (*A*). Screening of stem cell marker expression measured by flow cytometry in primary BM-MSC isolated from mice fed with ND or HFD over 12 weeks ($n = 6$). (*B*) Proliferative capacity of BM-MSC over 9 days in culture ($n = 4$–6). (*C*) Colony-forming unit properties, (*D*) senescence evaluation as SA-β gal activity per cell viability measurement, and (*E*) gene expression represented as fold change of senescence markers *p16* and *p21* in BM-MSC isolated from ND and HFD mice ($n = 4$–6). (*F*) Adipocyte differentiation potential of the BM-MSC evaluated by gene expression of *Pparγ2, Lep, Adipoq*, and *Fsp27*. (*G, H*) Osteoblast differentiation potential of the BM-MSC evaluated by quantification of (*G*) alkaline phosphatase (ALP) activity represented as fold change over noninduced cells (day 11) and (*H*) by gene expression of *Alp, Runx2*, and *Ocn* ($n = 4$–6). Data are presented as mean ± SEM from three independent experiments. $^{*}p < 0.05$, $^{**}p < 0.01$ compared with ND, two-tailed unpaired Student's *t* test.

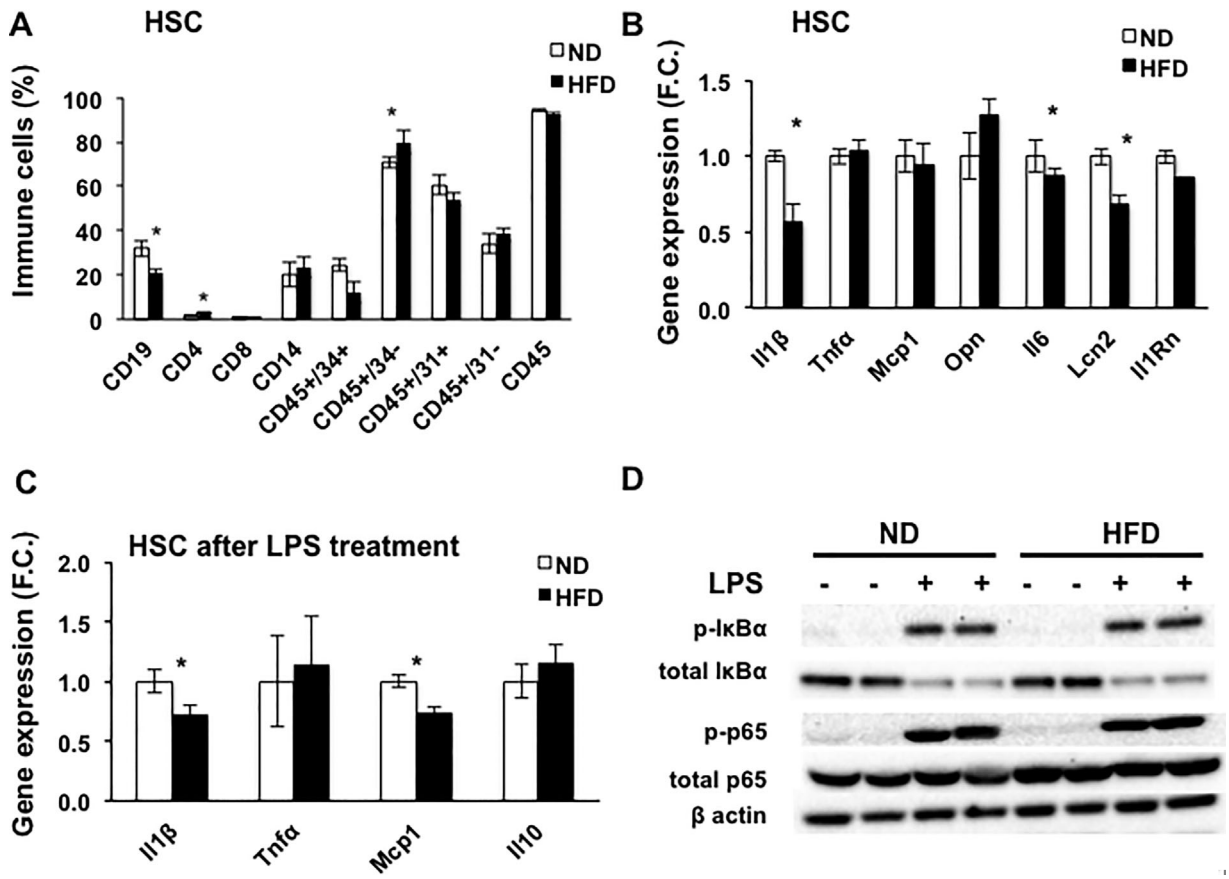

Fig. 4. HSC composition and their inflammatory status in HFD mice. (*A*) Immunophenotyping of hematopoietic stem cells (HSC) measured by flow cytometry in ND and HFD mice ($n = 3$). (*B*) Gene expression profile represented as fold change of inflammatory genes in HSC of mice fed for 20 weeks with ND or HFD directly after isolation ($n = 3$) (*C*) or after 3 hours of LPS treatment (100 ng/μL) ($n = 3$). (*D*) Representative Western blotting to evaluate phosphorylation of IκBα (p-IκB) and total IκBα and phosphorylation of p65 (p-p65) and total p65 after LPS exposure (15 minutes, 100 ng/μL) in HSC isolated from ND or HFD mice fed 20 weeks of HFD. Data are presented as mean ± SEM from three independent experiments. $^{*}p < 0.05$, compared with ND, two-tailed unpaired Student's *t* test.

Discussion

In the present study, we report that HFD-induced obesity in mice leads to increased BMAT formation, enhanced AD differentiation of BM-MSC, and reduced bone mass. Interestingly, BMAT, in contrast to extramedullary adipocytes, did not exhibit a pro-inflammatory phenotype and maintained its insulin responsiveness. Our study suggests that BMAT responds to metabolic stimuli and acts as a depot for storing extra energy during HFD when peripheral AT is incapable of mediating this function.

HFD-induced obesity led to decreased bone mass and BMAT expansion

Similar to other investigators studying BMAT in mice and humans, we observed that HFD increased BMAT formation as evidenced by increased BMAT volume, adipocyte number, and size.[3,4,33–37] In addition, we observed significant and consistent decrease in trabecular and cortical bone mass after 12 weeks of HFD. Previous studies have reported inconsistent results regarding the impact of HFD on bone mass and bone quality. Some studies reported no change or increased or decreased bone mass with lower bone strength.[33–36,38,39] These discrepancies can be explained by variations in experimental models, e.g., mouse strain, sex, length/type/composition of diet (60% versus 45% fat or 10% corn oil), and possibly evaluation methods. However, the consistency observed in our study and some of the previous studies,[35,37,40,41] as well as the recent study of Bornstein and colleagues reported HFD induced reduction in the cortical and trabecular parameters in the long bones along with increased BMAT volume,[37] suggesting that bone mass reduction is a biological consequence of coherent mechanisms of cellular and molecular changes relevant for studies of bone fragility in human obesity.[42–44]

HFD led to a progenitor cell "exhaustion" and enhanced adipocyte differentiation

BMAT originate from progenitor cell population within the BM stroma.[45,46] We observed that HFD-induced obesity increased BMAT volume and is associated with decreased proliferative potential of progenitor cells and enhanced differentiation of BM-MSC into adipocytes. Based on a number of pathophysiological studies, an inverse relationship between BMAT and bone

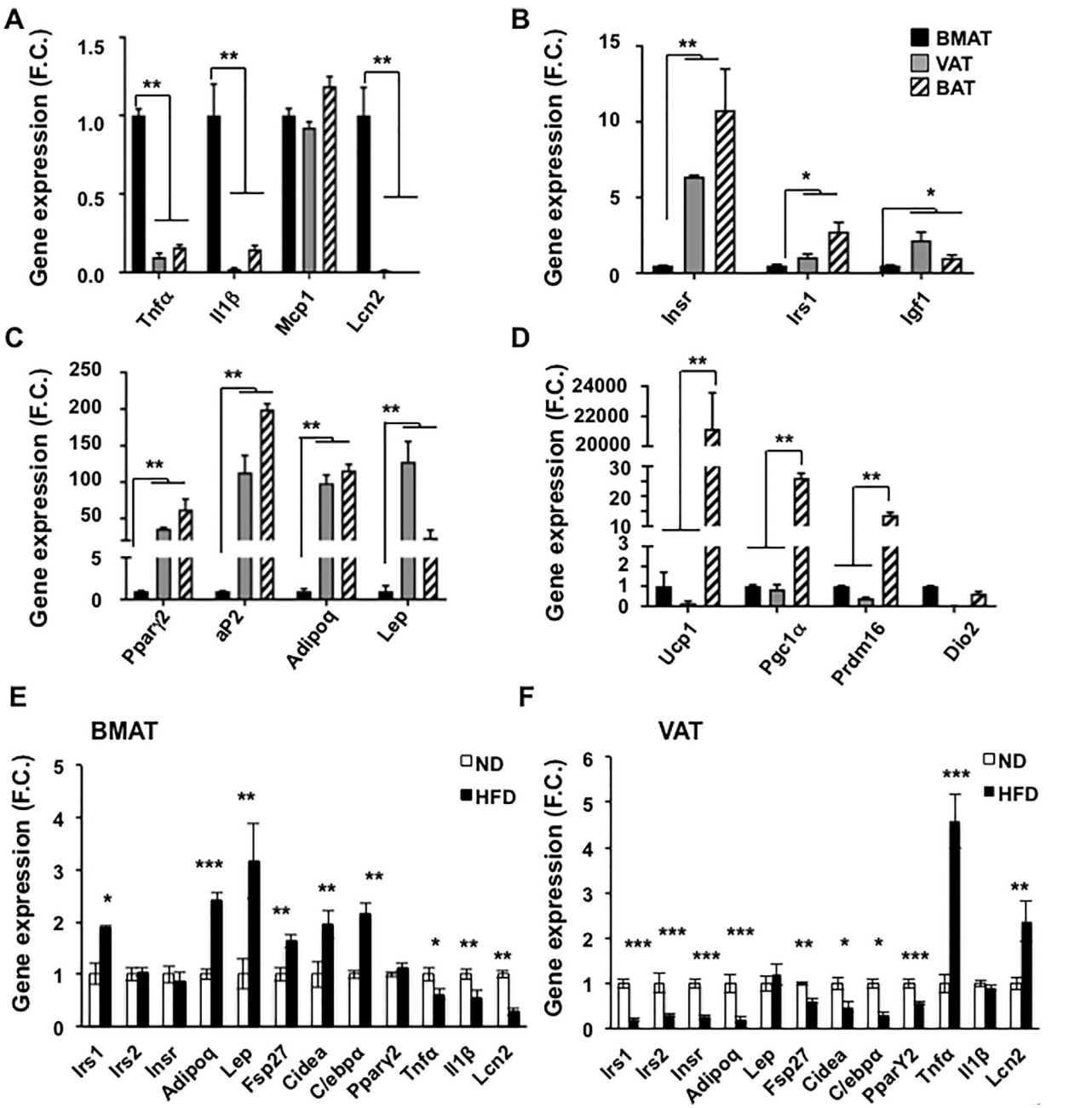

Fig. 5. BMAT gene expression profile compared with peripheral adipose depots in lean and HFD condition. (*A–D*) Gene expression profile in different adipose depots BMAT, VAT, and BAT in ND mice: (*A*) inflammatory genes as *Tnfα*, *Il1β*, *Mcp1*, and *Lcn2*, (*B*) insulin signaling-related genes as *Insr*, *Irs1*, *and Igf1*, (*C*) adipogenic genes as *Pparγ2*, *aP2*, *Adipoq*, and *Lep* and (*D*) brown fat-related genes as *Ucp1*, *Pgc1α*, *Prdm16*, and *Dio2* ($n = 3$). (*E*) Impact of 20 weeks of HFD on the gene expression profile in BMAT and (*F*) VAT ($n = 6$). Data are presented as mean ± SEM ($^{*}p < 0.05$, $^{**}p < 0.01$, $^{***}p < 0.001$: ND versus HFD, one-way analysis of variance (ANOVA) for *A–D* and two-tailed unpaired Student's *t* test for *E–F*).

formation has been reported,[3,4,47,48] suggesting changes in BM-MSC commitment to adipocyte versus osteoblast lineage.[49] Our data support this hypothesis under HFD-induced obesity, as we observed enhanced adipocyte differentiation in BM-MSC obtained from HFD mice. Moreover, decreased number of Sca1+ cells in HFD suggests that the expansion of adipocytic progenitors (Sca1-) might occur as previously reported.[50] The decrease in BM-MSC and increased number of committed adipocytes may be caused by several mechanisms including changes in the BM-MSC niche due to local and systemic changes[51] or high-triglyceride load in the circulation increasing lipid uptake by skeleton.[52]

HFD did not cause an "inflamed" BMAT

We examined for a possible mechanism that links obesity, BMAT expansion, and decreased bone mass. Obesity is associated with increased inflammation in peripheral AT.[1,22] Our results

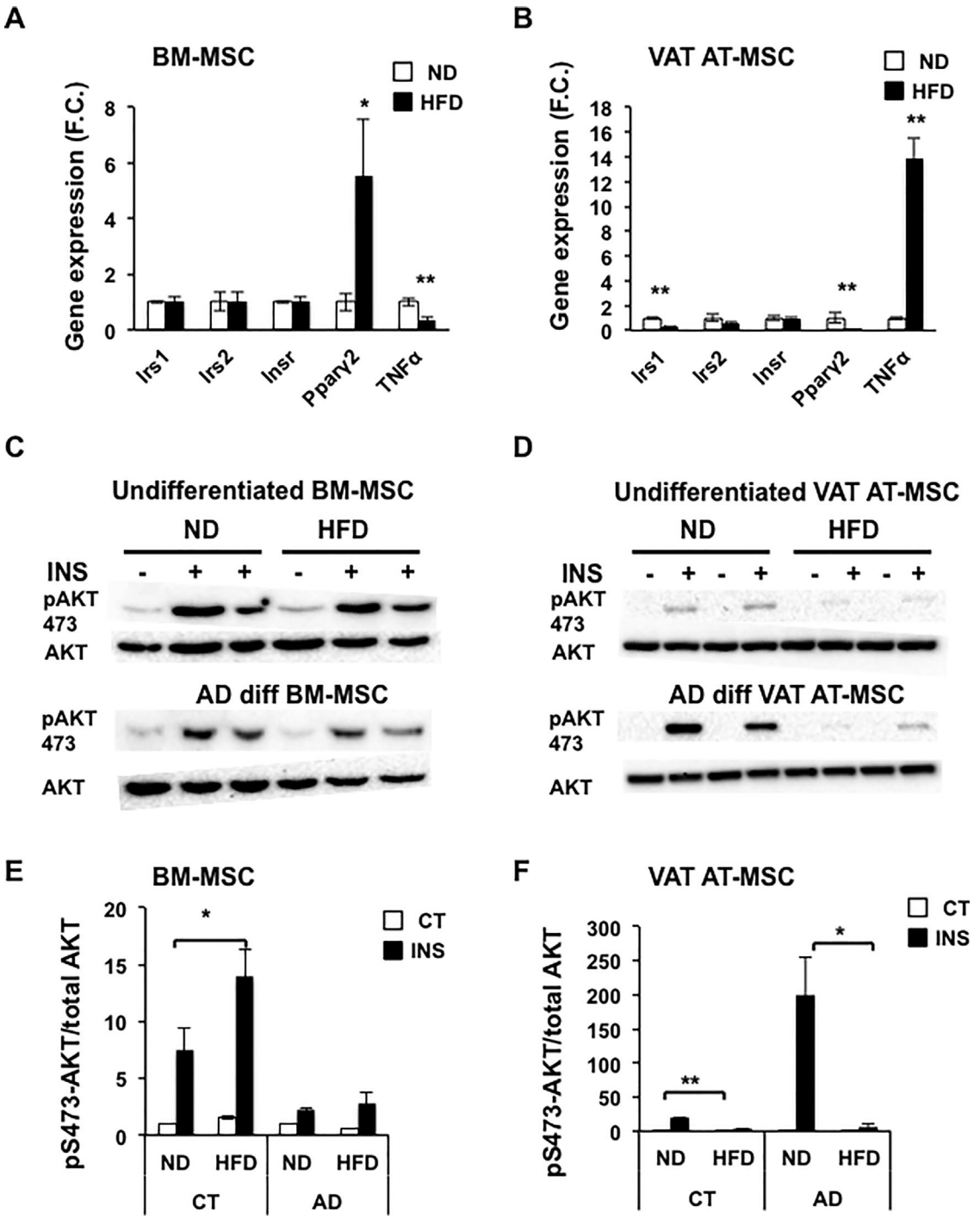

Fig. 6. Comparison of BM-MSC to AT-MSC in relation to adipogenesis and insulin responsiveness in HFD mice. Impact of HFD on the gene expression profile represented as fold change in (*A*) BM-MSC and (*B*) AT-MSC from VAT ($n = 3$). (*C*, *D*) Representative Western blot to evaluate insulin-stimulated (100 nM, 15 minutes) phosphorylation of AKT (p-S473AKT) and total AKT in undifferentiated and AD differentiated (*C*) BM-MSC and (*D*) AT-MSC from VAT ($n = 2$–3). (*E*, *F*) Densitometry evaluation of Western blot measuring insulin stimulation (100 nM) of AKT as p-S473-AKT/total AKT in undifferentiated and differentiated cells from (*E*) BM-MSC and (*F*) AT-MSC from VAT ($n = 2$–3). Data are presented as mean ± SEM from three independent experiments ($^{*}p < 0.05$, $^{**}p < 0.01$: ND versus HFD, two-tailed unpaired Student's *t* test).

demonstrated that after HFD, BMAT does not develop a "pro-inflammatory" phenotype similar to that observed in peripheral AT with impaired adipogenesis and insulin signaling along with increased inflammation.[22] In contrast to previous studies[20] that examined BMAT as part of the heterogeneous bone tissue, we isolated BMAT directly from long bones, which enhanced the internal validity of our study and point out that decreased bone mass is not the result of "inflamed" BMAT.

HFD did not lead to a "pro-inflammatory" BM microenvironment

BMAT and its progenitors exist within a close proximity to hematopoietic marrow. Previous studies reported obesity-induced impairment of hematopoiesis, including depletion of B lymphocytes and changes in HSC niche.[16,53,54] We observed decreased B lymphopoiesis and increased CD4+ T lymphocyte and CD45+/CD34- HSC populations in HFD mice. These changes may be attributed to changes in adipokine secretion, having inhibitory effects on HSC proliferation and differentiation.[17,19,50] *In vitro* studies showed that adipocyte-derived factors such as adiponectin could impair B lymphopoiesis and increase myelopoiesis.[55,56] Indeed, in our study, we observed increased levels of adiponectin in BMAT along with decreased B-lymphocyte population. In addition, LPS responsiveness in HSC exposed to the HFD environment was impaired, suggesting the presence of a "protective" mechanism against BM inflammation during the initial phases of BMAT expansion in obesity. Future studies need to determine the anti-inflammatory mechanisms and its relevance to the BMAT biology.

BMAT maintains an insulin-responsive phenotype in HFD-induced obesity

The physiology of BMAT and its contribution to whole-body metabolism is still not well understood. In the present study, the molecular and cellular data on BMAT phenotype with increased expression of insulin-responsive genes raised a question whether BMAT insulin signaling is affected by obesity similar to peripheral AT. Recent animal studies revealed that insulin-regulated glucose uptake in the skeleton measured by PET scanning was decreased under HFD, suggesting the presence of insulin resistance.[23,24,57] However, in these studies, they did not distinguish BMAT from the rest of the BM. Our findings in BMSC and BMAT point out that BMAT is a "metabolically responsive" tissue in HFD, and contrary to peripheral extramedullary AT, it may respond to increased metabolic demand coming from the BM microenvironment and serves as a buffering organ for excessive energy. However, longer exposure to HFD might switch the BMAT metabolic phenotype with a worse impact on bone. This needs to be addressed in future studies.

There are some limitations in our study. First, there may be a risk that the isolated BMAT preparations were contaminated with hematopoietic cells, which affects the molecular analysis of BMAT phenotype. However, we observed no difference in the number of CD45+ cells in BMAT preparations obtained from ND and HFD mice, suggesting the absence of significant hematopoietic cell contamination. The presence of hematopoietic cells would have increased the levels of pro-inflammatory cytokines, whereas we observed a decrease in their levels. Second, we employed collagenase digestion in cell isolation procedures, which may activate several inflammatory pathways. However, we employed collagenase isolation in both BM-MSC and AT-MSC, and the cells were cultured under identical conditions for several days, minimizing the confounding effects of collagenase on inflammation-associated gene expression. Third, in our study, we employed male mice because they are more prone to obesity-induced metabolic complications.[58,59] However, studies of female mice need to be performed to generalize our findings.

HFD-induced obesity in mice led to decreased bone mass, which is different from the observed increase in bone mass in obese humans, limiting the translational relevance of our study. However, BMAT expansion is a consistent finding in HFD mice

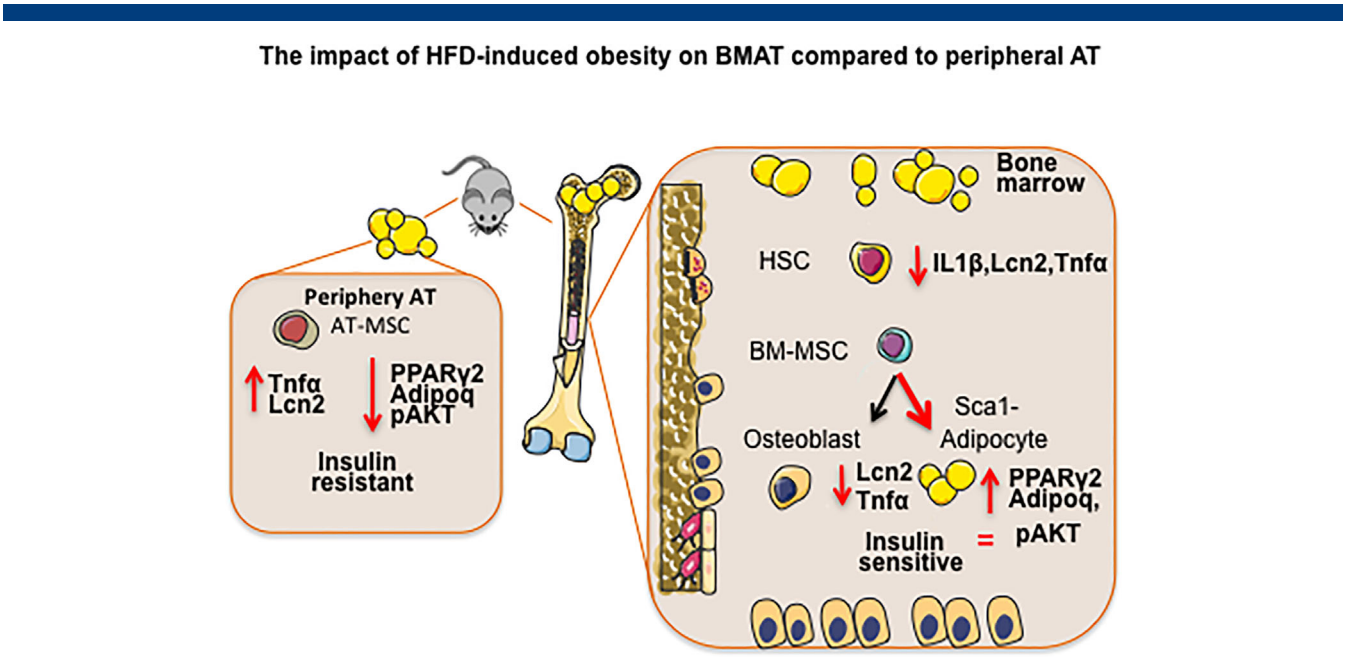

Fig. 7. A working model for the effects of HFD-induced obesity on BMAT compared with peripheral AT. In HFD condition and compared with peripheral adipose tissue (AT), bone marrow microenvironment exhibits decreased inflammatory response of hematopoietic cells (HC) and adipocytic progenitors as well as maintenance of insulin signaling leading to enhanced adipogenesis. Peripheral AT exhibits higher levels of inflammation and impaired insulin signaling. The BMAT expansion can thus serve to buffer excess energy from HFD. This results in decreased osteoblast recruitment and consequently decreased bone formation.

and in obese humans.[4,60] Thus, our study is relevant to the understanding the cellular, molecular, and metabolic consequences of increased bone marrow adipogenesis and provides insight into the possible mechanisms of bone fragility observed in obese humans.

In summary (Fig. 7), the present study proposes a model for the relationship between increased BMAT and decreased bone mass after HFD feeding. The absence of inflammation and continuous recruitment of pre-adipocytic cells from BM-MSC to buffer the excess calories leads to stem cell exhaustion and impaired osteoblast recruitment and bone formation. Importantly, our findings demonstrate the presence of a metabolically healthy BMAT capable of responding to metabolic demands in a low-inflammatory BM microenvironment, which is opposite to what is observed in peripheral AT, suggesting an unexpected role of BMAT in obesity and providing possible strategies for a treatment of obesity-induced bone fragility.

Disclosures

All authors state that they have no conflicts of interest.

Acknowledgments

The authors are grateful to Bianca Jørgensen and Catherine Reilly for excellent technical assistance. We thank professor Cliff Rosen for helpful discussions and suggestions. This work was supported by a fellowship grant from the Danish Diabetes Academy supported by the Novo Nordisk Foundation (MT) and the Novo Nordisk Foundation (MK, NNF15OC0016284) and a research grant from the Odense University Hospital (R29-A1374).

Authors' roles: MT and MK conceived the project. MT, FF, ND, and TKN performed the in vitro and in vivo experiments. HT performed dynamic bone histomorphometry. MT, FF, ND, and TKN collected and analyzed data. MT, FF, and MK designed and supervised the study and wrote the manuscript. All authors revised and approved the manuscript. MT takes responsibility for the integrity of the data analysis.

References

1. Guilherme A, Virbasius JV, Puri V, Czech MP. Adipocyte dysfunctions linking obesity to insulin resistance and type 2 diabetes. Nat Rev Mol Cell Biol. 2008;9(5):367–77.
2. Gonnelli S, Caffarelli C, Nuti R. Obesity and fracture risk. Clin Cases Miner Bone Metab. 2014;11(1):9–14.
3. Bredella MA, Gill CM, Keating LK, et al. Assessment of abdominal fat compartments using DXA in premenopausal women from anorexia nervosa to morbid obesity. Obesity (Silver Spring). 2013;21(12): 2458–64.
4. Bredella MA, Torriani M, Ghomi RH, et al. Vertebral bone marrow fat is positively associated with visceral fat and inversely associated with IGF-1 in obese women. Obesity (Silver Spring). 2011;19(1):49–53.
5. Fazeli PK, Ackerman KE, Pierce L, Guereca G, Bouxsein M, Misra M. Sclerostin and Pref-1 have differential effects on bone mineral density and strength parameters in adolescent athletes compared with non-athletes. Osteoporos Int. 2013;24(9):2433–40.
6. Cawthorn WP, Scheller EL, Learman BS, et al. Bone marrow adipose tissue is an endocrine organ that contributes to increased circulating adiponectin during caloric restriction. Cell Metab. 2014;20(2): 368–75.
7. Gimble JM, Floyd ZE, Kassem M, Nuttall ME. Aging and bone. In: Duque G, Kiel DP, editors. *Osteoporosis in older persons: advances in pathophysiology and therapeutic approaches*. 2nd ed. Gewerbestrasse, Switzerland: Springer; 2016. p. 23–42.
8. Lecka-Czernik B. Bone loss in diabetes: use of antidiabetic thiazolidinediones and secondary osteoporosis. Curr Osteoporos Rep. 2010;8(4):178–84.
9. Tencerova M, Kassem M. The bone marrow-derived stromal cells: commitment and regulation of adipogenesis. Front Endocrinol (Lausanne). 2016;7:127.
10. Gilbert L, He X, Farmer P, et al. Inhibition of osteoblast differentiation by tumor necrosis factor-alpha. Endocrinology. 2000;141(11): 3956–64.
11. Hamam D, Ali D, Kassem M, Aldahmash A, Alajez NM. microRNAs as regulators of adipogenic differentiation of mesenchymal stem cells. Stem Cells Dev. 2015;24(4):417–25.
12. Yu B, Zhao X, Yang C, et al. Parathyroid hormone induces differentiation of mesenchymal stromal/stem cells by enhancing bone morphogenetic protein signaling. J Bone Miner Res. 2012; 27(9):2001–14.
13. Guntur AR, Rosen CJ. IGF-1 regulation of key signaling pathways in bone. Bonekey Rep. 2013;2:437.
14. Abdallah BM, Jensen CH, Gutierrez G, Leslie RG, Jensen TG, Kassem M. Regulation of human skeletal stem cells differentiation by Dlk1/ Pref-1. J Bone Miner Res. 2004;19(5):841–52.
15. Abdallah BM, Kassem M. New factors controlling the balance between osteoblastogenesis and adipogenesis. Bone. 2012;50(2): 540–5.
16. Adler BJ, Kaushansky K, Rubin CT. Obesity-driven disruption of haematopoiesis and the bone marrow niche. Nat Rev Endocrinol. 2014;10(12):737–48.
17. Naveiras O, Nardi V, Wenzel PL, Hauschka PV, Fahey F, Daley GQ. Bone-marrow adipocytes as negative regulators of the haematopoietic microenvironment. Nature. 2009;460(7252):259–63.
18. Trottier MD, Naaz A, Li Y, Fraker PJ. Enhancement of hematopoiesis and lymphopoiesis in diet-induced obese mice. Proc Natl Acad Sci U S A. 2012;109(20):7622–9.
19. Zhou BO, Yu H, Yue R, et al. Bone marrow adipocytes promote the regeneration of stem cells and haematopoiesis by secreting SCF. Nat Cell Biol. 2017;19(8):891–903.
20. Krings A, Rahman S, Huang S, Lu Y, Czernik PJ, Lecka-Czernik B. Bone marrow fat has brown adipose tissue characteristics, which are attenuated with aging and diabetes. Bone. 2012;50(2):546–52.
21. Devlin MJ, Cloutier AM, Thomas NA, et al. Caloric restriction leads to high marrow adiposity and low bone mass in growing mice. J Bone Miner Res. 2010;25(9):2078–88.
22. Czech MP, Tencerova M, Pedersen DJ, Aouadi M. Insulin signalling mechanisms for triacylglycerol storage. Diabetologia. 2013;56(5) :949–64.
23. Huovinen V, Saunavaara V, Kiviranta R, et al. Vertebral bone marrow glucose uptake is inversely associated with bone marrow fat in diabetic and healthy pigs: [(18)F]FDG-PET and MRI study. Bone. 2014;61:33–8.
24. Zoch ML, Abou DS, Clemens TL, Thorek DL, Riddle RC. In vivo radiometric analysis of glucose uptake and distribution in mouse bone. Bone Res. 2016;4:16004.
25. Ding M, Danielsen CC, Hvid I. Age-related three-dimensional microarchitectural adaptations of subchondral bone tissues in guinea pig primary osteoarthrosis. Calcif Tissue Int. 2006;78(2): 113–22.
26. Houlihan DD, Mabuchi Y, Morikawa S, et al. Isolation of mouse mesenchymal stem cells on the basis of expression of Sca-1 and PDGFR-alpha. Nat Protoc. 2012;7(12):2103–11.
27. Zhu H, Guo ZK, Jiang XX, et al. A protocol for isolation and culture of mesenchymal stem cells from mouse compact bone. Nat Protoc. 2010;5(3):550–60.
28. Lanske B, Rosen C. Bone marrow adipose tissue: the first 40 years. J Bone Miner Res. 2017;32(6):1153–6.
29. Liu Y, Wang L, Kikuiri T, et al. Mesenchymal stem cell-based tissue regeneration is governed by recipient T lymphocytes via IFN-gamma and TNF-alpha. Nat Med. 2011;17(12):1594–601.
30. Dempster DW, Compston JE, Drezner MK, et al. Standardized nomenclature, symbols, and units for bone histomorphometry: a

2012 update of the report of the ASBMR Histomorphometry Nomenclature Committee. J Bone Miner Res. 2013;28(1):2–17.

31. Parfitt AM, Drezner MK, Glorieux FH, et al. Bone histomorphometry: standardization of nomenclature, symbols, and units. Report of the ASBMR Histomorphometry Nomenclature Committee. J Bone Miner Res. 1987;2(6):595–610.
32. Aouadi M, Tencerova M, Vangala P, et al. Gene silencing in adipose tissue macrophages regulates whole-body metabolism in obese mice. Proc Natl Acad Sci U S A. 2013;110(20):8278–83.
33. Doucette CR, Horowitz MC, Berry R, et al. A high fat diet increases bone marrow adipose tissue (MAT) but does not alter trabecular or cortical bone mass in C57BL/6J mice. J Cell Physiol. 2015;230(9): 2032–7.
34. Halade GV, Rahman MM, Williams PJ, Fernandes G. High fat diet-induced animal model of age-associated obesity and osteoporosis. J Nutr Biochem. 2010;21(12):1162–9.
35. Scheller EL, Khoury B, Moller KL, et al. Changes in skeletal integrity and marrow adiposity during high-fat diet and after weight loss. Front Endocrinol (Lausanne). 2016;7:102.
36. Styner M, Pagnotti GM, McGrath C, et al. Exercise decreases marrow adipose tissue through ß-oxidation in obese running mice. J Bone Miner Res. 2017;32(8):1692–702.
37. Bornstein S, Moschetta M, Kawano Y, et al. Metformin affects cortical bone mass and marrow adiposity in diet-induced obesity in male mice. Endocrinology. 2017;158(10):3369–85.
38. Devlin MJ, Van Vliet M, Motyl K, et al. Early-onset type 2 diabetes impairs skeletal acquisition in the male TALLYHO/JngJ mouse. Endocrinology. 2014;155(10):3806–16.
39. Lecka-Czernik B, Stechschulte LA, Czernik PJ, Dowling AR. High bone mass in adult mice with diet-induced obesity results from a combination of initial increase in bone mass followed by attenuation in bone formation; implications for high bone mass and decreased bone quality in obesity. Mol Cell Endocrinol. 2015;410:35–41.
40. Cao JJ, Sun L, Gao H. Diet-induced obesity alters bone remodeling leading to decreased femoral trabecular bone mass in mice. Ann N Y Acad Sci. 2010;1192:292–7.
41. Patsch JM, Kiefer FW, Varga P, et al. Increased bone resorption and impaired bone microarchitecture in short-term and extended high-fat diet-induced obesity. Metabolism. 2011;60(2):243–9.
42. Fajardo RJ, Karim L, Calley VI, Bouxsein ML. A review of rodent models of type 2 diabetic skeletal fragility. J Bone Miner Res. 2014;29(5):1025–40.
43. Goulding A, Taylor RW, Jones IE, McAuley KA, Manning PJ, Williams SM. Overweight and obese children have low bone mass and area for their weight. Int J Obes Relat Metab Disord. 2000;24(5):627–32.
44. Junior IF, Cardoso JR, Christofaro DG, Codogno JS, de Moraes AC, Fernandes RA. The relationship between visceral fat thickness and bone mineral density in sedentary obese children and adolescents. BMC Pediatr. 2013;13:37.
45. Rosen CJ, Klibanski A. Bone, fat, and body composition: evolving concepts in the pathogenesis of osteoporosis. Am J Med. 2009; 122(5):409–14.
46. Gimble JM, Robinson CE, Wu X, Kelly KA. The function of adipocytes in the bone marrow stroma: an update. Bone. 1996;19(5):421–8.
47. Bredella MA, Fazeli PK, Miller KK, et al. Increased bone marrow fat in anorexia nervosa. J Clin Endocrinol Metab. 2009;94(6):2129–36.
48. Rzonca SO, Suva LJ, Gaddy D, Montague DC, Lecka-Czernik B. Bone is a target for the antidiabetic compound rosiglitazone. Endocrinology. 2004;145(1):401–6.
49. Gimble JM, Zvonic S, Floyd ZE, Kassem M, Nuttall ME. Playing with bone and fat. J Cell Biochem. 2006;98(2):251–66.
50. Ambrosi TH, Scialdone A, Graja A, et al. Adipocyte accumulation in the bone marrow during obesity and aging impairs stem cell-based hematopoietic and bone regeneration. Cell Stem Cell. 2017;20-(6):771–84 e6.
51. Greenberg AS, Obin MS. Obesity and the role of adipose tissue in inflammation and metabolism. Am J Clin Nutr. 2006;83(2):461S–5S.
52. Bartelt A, Koehne T, Todter K, et al. Quantification of bone fatty acid metabolism and its regulation by adipocyte lipoprotein lipase. Int J Mol Sci. 2017;18(6).
53. Chan ME, Adler BJ, Green DE, Rubin CT. Bone structure and B-cell populations, crippled by obesity, are partially rescued by brief daily exposure to low-magnitude mechanical signals. FASEB J. 2012; 26(12):4855–63.
54. Yang H, Youm YH, Vandanmagsar B, et al. Obesity accelerates thymic aging. Blood. 2009;114(18):3803–12.
55. Bilwani FA, Knight KL. Adipocyte-derived soluble factor(s) inhibits early stages of B lymphopoiesis. J Immunol. 2012;189(9):4379–86.
56. Yokota T, Meka CS, Kouro T, et al. Adiponectin, a fat cell product, influences the earliest lymphocyte precursors in bone marrow cultures by activation of the cyclooxygenase-prostaglandin pathway in stromal cells. J Immunol. 2003;171(10):5091–9.
57. Heinonen I, Kemppainen J, Kaskinoro K, et al. Bone blood flow and metabolism in humans: effect of muscular exercise and other physiological perturbations. J Bone Miner Res. 2013;28(5):1068–74.
58. Hwang LL, Wang CH, Li TL, et al. Sex differences in high-fat diet-induced obesity, metabolic alterations and learning, and synaptic plasticity deficits in mice. Obesity (Silver Spring). 2010;18(3):463–9.
59. Pettersson US, Walden TB, Carlsson PO, Jansson L, Phillipson M. Female mice are protected against high-fat diet induced metabolic syndrome and increase the regulatory T cell population in adipose tissue. PLoS One. 2012;7(9):e46057.
60. Bredella MA, Torriani M, Ghomi RH, et al. Determinants of bone mineral density in obese premenopausal women. Bone. 2011;48(4): 748–54.